

# Specimen design for low-cycle fatigue experiments under large strain amplitude loading

J. Fumfera <sup>1,a</sup>, R. Procházka <sup>2</sup>

<sup>1</sup> *Czech Technical University in Prague, Faculty of Mechanical Engineering, Department of Mechanics, Biomechanics and Mechatronics, Technická 4, 166 07 Praha 6, Czech Republic*

<sup>2</sup> *COMTES FHT a.s., Průmyslová 995, 334 41 Dobřany, Czech Republic*

<sup>a</sup> *jaromir.fumfera@fs.cvut.cz*

**Abstract:** Specimen design for uniaxial low-cycle fatigue test of 08Ch18N10T austenitic steel under large strain amplitude (up to 3%) loading conditions is presented. Design phase FEM analysis including post-buckling analysis with inclusion of non-linear material plasticity is presented. New axisymmetric specimen design based on meridian section of elliptical shape is introduced. Some details about experimental equipment and experimental results are presented.

**Keywords:** Low-Cycle Fatigue, Large Strain Amplitude Experiments, Specimen Design

## 1 Introduction

Low-cycle fatigue (LCF) is a part of fatigue phenomenon, where loading implies higher nominal stresses than yield stress. Maximum number of cycles to failure for common steel-like materials is usually thousands of cycles or less [1]. Due to large stresses and strains in material, effects like post-buckling and additional bend can occur. The higher the loading amplitude is, the more obvious are these effects and specimen design must reflect these phenomena.

LCF experiments are usually strain-controlled. Deformations are measured for example by extensometer attached to a specimen's surface and applied load is feedback controlled by required value of extensometer's displacement. This type of controlling induces strain field in specimen. Usually there is required specific value of total strain amplitude in specific point or area. For 1D tests, bar specimens with uniform-gage test section (hereinafter "uniform-gage specimen") or specimen with variable longitudinal test section (i.e. hourglass specimens) are used [2]. Test are performed on different strain amplitude levels of total strain in test section.

Typical low-cycle fatigue life of 08Ch18N10T austenitic stainless steel presented in this paper usually shows initial cyclic hardening followed by saturation of cyclic deformation curve (stress-strain response of next cycle is almost the same as previous one). For larger strain amplitudes, cyclic hardening (or sometimes softening) can occur for some types of materials. Last stage shows cyclic softening due to degradation of material properties and crack growth up to final failure [3].

## 2 Specimens Design

### 2.1 Original specimen design

For the first series of experiments, uniform-gage specimen was used (see Fig. 1). Ex-post analysis of results shows that almost all uniform-gage specimens fail outside the test section in radius notch (that also means outside extensometer tips that control loading).

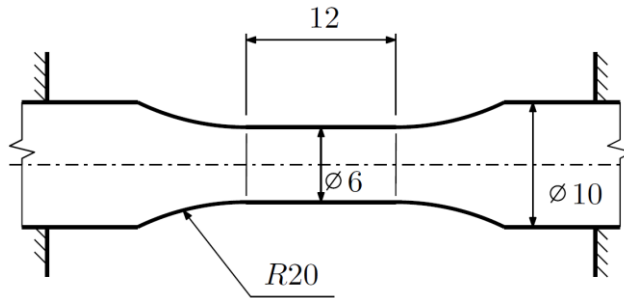


Fig. 1: Original uniform-gage specimen

Data analysis also shows different history of material hardening than expected. For almost all specimens, there is no material cyclic softening in the final stage (see Fig. 2). That indicates different type and cause of failure than expected. Finally, data analysis shows loss of stability control due to post buckling effect of several specimens under the highest strain amplitudes. Due to all these reasons, it was decided to propose new specimen design.

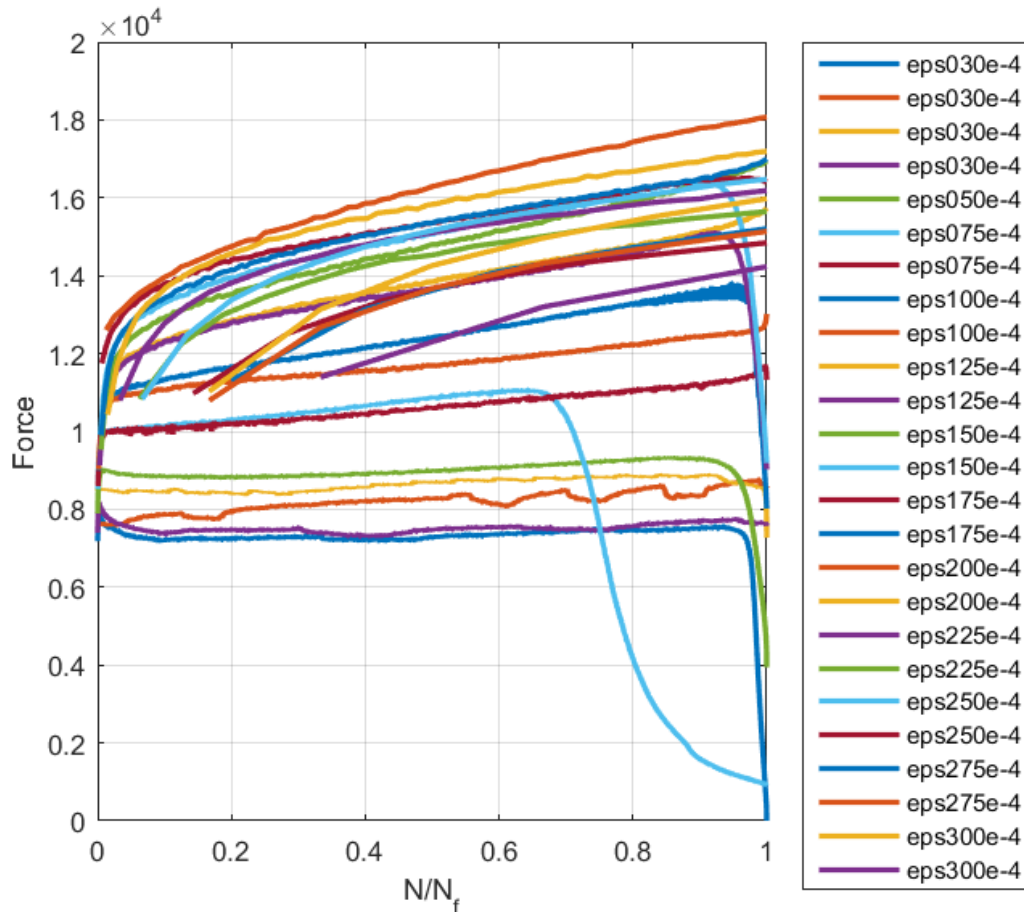


Fig. 2: Force progress during fatigue life for original uniform-gage specimen.  $N_f$  represents number of cycles at failure. See no-cyclic softening in the end of the fatigue life for almost all specimens.

## 2.2 New specimen design

Two candidates for new specimen design was proposed, both with variable longitudinal-section. This type of geometry localizes deformation into one cross-section (in the narrowest part) and also should be more post buckling-resistant. First specimen has circular longitudinal section (and is usually called hourglass specimen, see Fig. 3a), second one has elliptical longitudinal section (see Fig. 3b). Both specimens' dimensions are limited by experimental equipment and material cast.

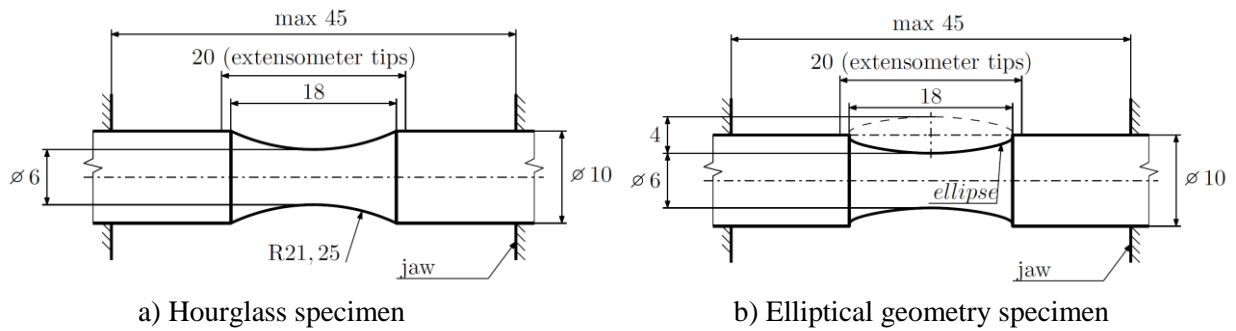


Fig. 3: New specimens suitable for LCF experiments under large strain range.

### 3 Design Phase Analyses

Series of Finite element method (FEM) simulation in FEM software Abaqus was done to analyze suitability and loading conditions of both newly proposed geometries.

#### 3.1 Post-Buckling Analysis

Research team was not looking for the real cause<sup>1</sup> of loss of stability control due to post-buckling effect. Problems with stability control occurs only on the highest loaded specimens (for total strain amplitude  $\epsilon_a = 2,75\% - 3\%$ ). Proposed post-buckling analysis should only estimate whether new specimen design is more post-buckling resistant than the original one.

Proposed procedure consists of two steps. First, specimen's geometrical imperfection, modelled as the first eigenmode (of sine shape, see Fig. 4), as maximum manufacturing tolerance was imported into FEM model as well as maximum allowed axis misalignment of experimental device. In second step, specimen FEM model is loaded by forced displacement in axial direction. Criterion for determination of the limit reaction force is chosen as transversal displacement of the specimen by 0,5 mm. Material model includes non-linear plasticity behavior and is approximated from static tensile curve.

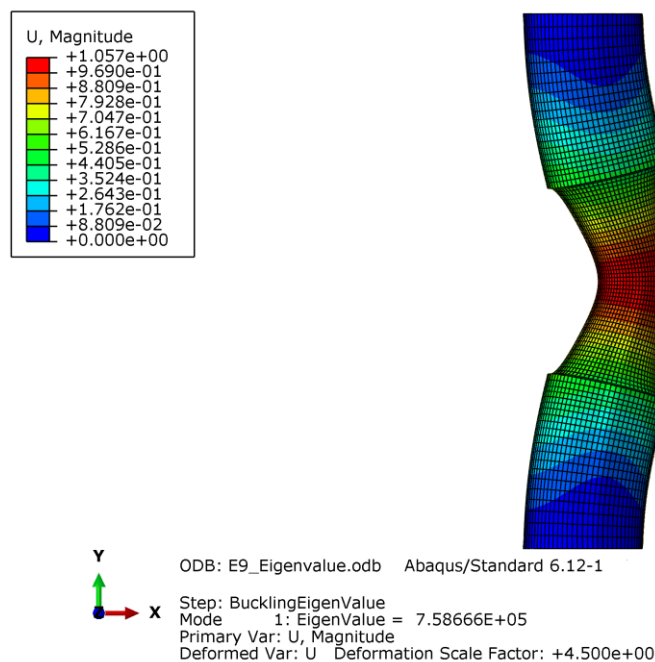


Fig. 4: Scaled initial imperfection of specimen.

<sup>1</sup> Origin of imperfection can be technological, caused by some non-isotropical material behavior, or caused by crack growth on one side of specimen...

### 3.2 Strain Field Analysis

Unlike the uniform-gage specimen, dependency between axial total strain amplitude and extensometer's displacement for specimen with variable longitudinal section is not trivial. Strain field analysis finds relationship between displacement of the extensometer's attached points and value of total strain amplitude on the surface of specimen in the narrowest point of specimen (point with highest deformation level, where crack usually starts to grow).

FEM simulation on the number of different load levels is performed and total axial strain amplitude value as a function of extensometer displacement is determined.

### 3.3 Triaxiality Factor Analysis

Triaxiality factor (hereinafter triaxiality) is dimensionless parameter defined as

$$TF = \frac{\sigma_{hydro}}{\sigma_{Mises}} \quad (1)$$

where  $\sigma_{hydro}$  is hydrostatic stress and  $\sigma_{Mises}$  is Mises equivalent stress (also known as HMH stress). It characterises stress field and for example the value of triaxiality for pure tension is  $TF = \frac{1}{3}$ . The purpose of this type of analysis is to check whether the stress field in analyzed variable geometries of specimens is approximately comparable with smooth specimen.

## 4 Analyses results

Results of post-buckling analysis are in Tab 1. It shows that proposed geometries can handle about 20% higher load, so they are significantly more post-buckling resistant. Again - it would be good to mention that these results should only be taken as a relative comparison of post-buckling resistance of presented geometries rather than exact procedure of determination of a limit loading.

Tab. 1: Post-buckling analysis results

Specimen Geometry	Limit Force [kN]
Uniform-gage (original)	17700
Hourglass	22700
Elliptical	22000

Strain field analysis of both specimen shows slightly non-linear dependency between extensometer's displacement and total strain amplitude value (see Fig. 5, Fig. 6).

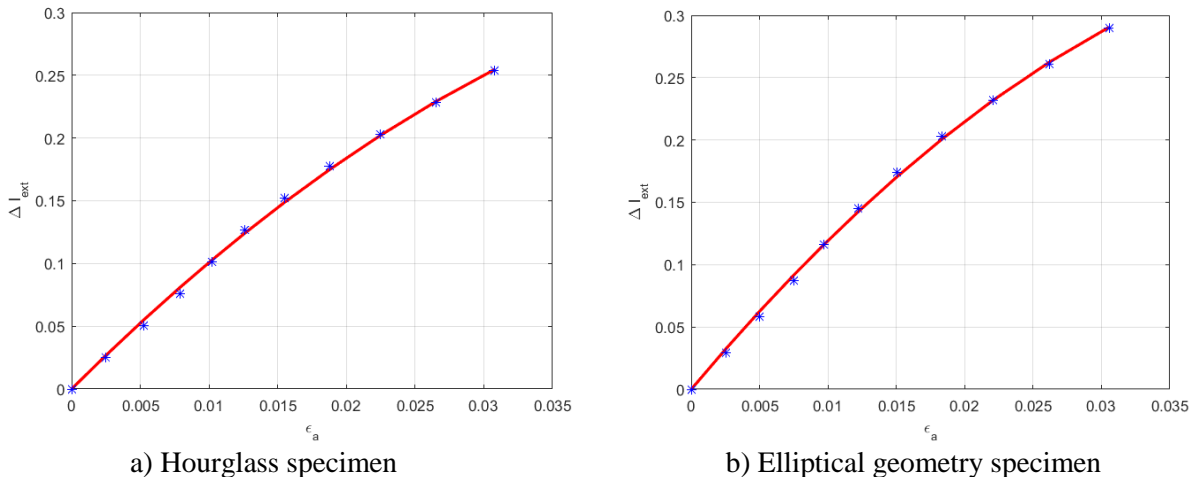


Fig. 5: Dependency of extensometer's displacement on axial strain amplitude.

Results of triaxiality analysis are in Fig. 6 and show very good agreement with the original uniform-gage specimen. The elliptical geometry shows values of triaxiality slightly closer to the original one.

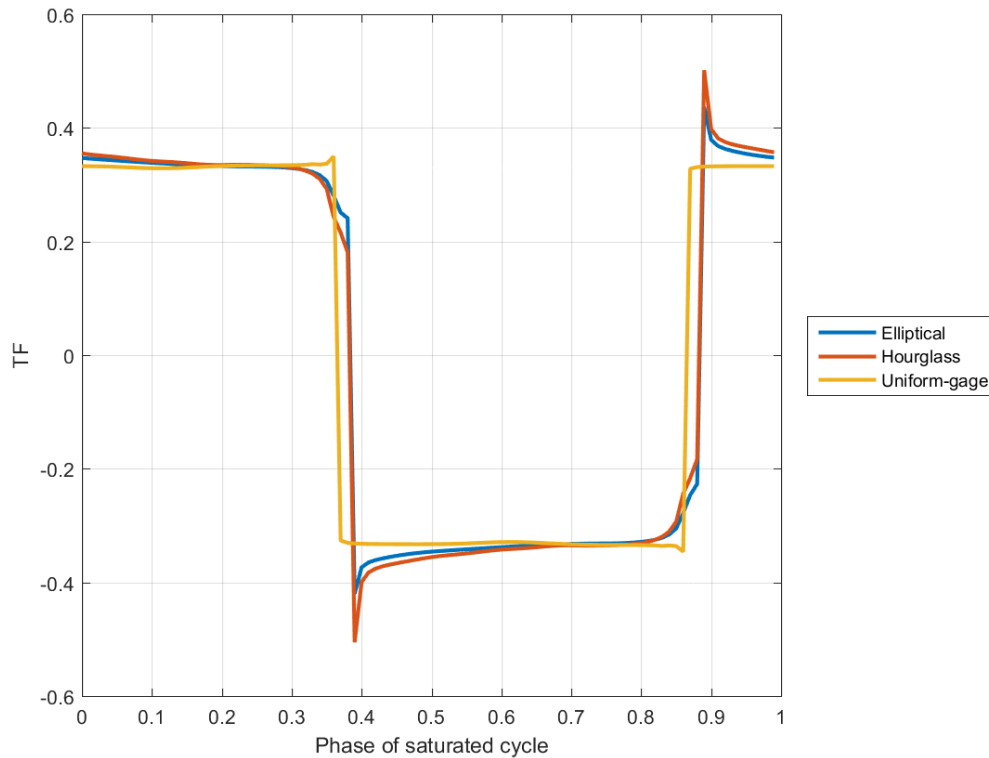


Fig. 6: Progress of triaxiality (TF) during saturated cycle.

All analyses show, that both proposed geometries should be suitable for LCF experiments even for large strain amplitude loading. Finally, it was decided to use elliptical geometry, because it's stress triaxiality parameter closer to the uniform-gage specimen.

## 5 Experiment

### 5.1 Experiment description

Tests were carried out by means of a computer-controlled electromechanical Mates machine with 100 kN capacity employing the LabControl software tool. The maximum stroke is 150mm. The base is not equipped with MTS Series 609 Alignment Fixture to reduce bending strains by improving concentric. Therefore, the test facility was adjusted for alignment fixture assembly which is mounted between the load cell and the load frame. Fatigue specimens were placed in the 647.25A side-loading hydraulic wedge grips (vee-shaped wedges). Constant strain amplitudes were controlled by the extensometer MTS model 634.25 with initial gauge length of 10mm with a 50% measuring range, in case of prismatic specimens, and length of 20mm with a 20% measuring range, in case of elliptical geometry specimens. The MTS model 650.03 extensometer calibrator was employed to get high accuracy at the lower strain levels where the data is more important. The calibration of the extensometer was done before and after each test program in accordance with ASTM E606 standard [1].

Fatigue tests were carried out on round and elliptical geometry specimens at constant strain amplitudes from 0.5% up to 3% of total deformation at ambient temperature. The load ratio of -1 was applied. The frequency of testing relates directly to the strain level at which the specimen was loaded. To keep a strain rate ( $0.002s^{-1}$ ) factor negligible and constant, the triangular waveform of the loading was used along with low loading frequencies. To reduce the influence of knife edges of contact extensometer, which is directly mounted on the specimen surface in gauge length area, the dull edges were used.

Each test was terminated after the specimen was separated. Fatigue tests were evaluated after the tensile force amplitude dropped 20% from the maximum of the force response.

Furthermore, the attention is paid to keep the fracture surface of the specimen in good condition for additional fractography investigations. Consequently, the crosshead software limits had to be set to avoid damaging fatigue crack surfaces which may lead to make the observation impossible.



Fig. 6: Experimental setup includes extensometer and hydraulic wedge grips.

## 5.2 Experiment Results

Experimental results confirm, that elliptical geometry has no tendency to post-buckle and force progress during fatigue life is in accordance with expectations (see Fig. 7).

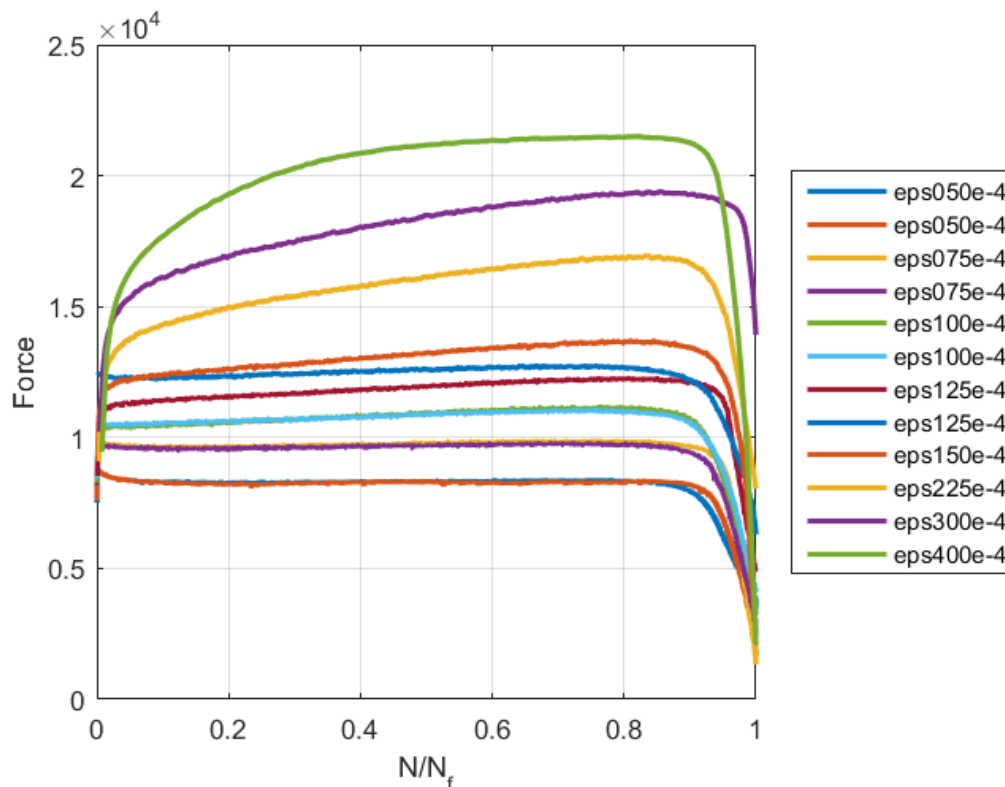


Fig. 7: Force progress during fatigue life for elliptical geometry specimen.

## 6 Conclusion

Unsuitability of originally used uniform-gage specimens was briefly analyzed. Two new geometry designs of specimens' candidates were proposed. Post-buckling, strain field and triaxiality analysis was done. Elliptical geometry specimen was chosen because of better triaxiality factor progress. Subsequent experimental procedure was described. Experimental results proved buckling resistance of new elliptical geometry design and force progress during fatigue life in accordance with expectations.

## Acknowledgement

The authors would like to acknowledge support from the Technology Agency of the Czech Republic, grant No. TA04020806, and support from the Grant Agency of the Czech Technical University in Prague, grant No. SGS15/187/OHK2/3T/12.

## References

- [1] Lemaitre, J. and Desmorat, Rodrigue. Engineering Damage Mechanics. New York: Springer, 2005. ISBN 3-540-21503-4.
- [2] American Society for Testing and Materials. Standard practice for strain-controlled fatigue testing, E606-04. ASM International: The Materials Information Society; 2004.
- [3] Fekete, B.: Isothermal and thermal–mechanical fatigue of VVER-440 reactor pressure vessel steels. Journal of Nuclear Materials 464, 2015.
- [4] Fumfera, J.: Návrh vzorků a parametrů zatežování. Zpráva ČVUT FS č. 12105/15/02, 2015.